Radial integrals for the magnetic form factor of the 5d electrons of rare earth elements

Kohjiro Kobayashi,[a]* Tatsuya Nagao[b] and Masahisa Ito[b]

[a]Advanced Technology Research Center, Gunma University, 1-5-1 Tenjin-cho, Kiryu, Gunma, 376-8515, Japan, and [b]Graduate School of Engineering, Gunma University, 1-5-1 Tenjin-cho, Kiryu, Gunma, 376-8515, Japan. Correspondence e-mail: kobablue@gmail.com

The radial integrals $\langle j_L \rangle$, where $L = 0, 2, 4$, for several electronic configurations of the 5d electrons of rare earth elements are calculated using radial wavefunctions from the Hartree–Fock relativistic method in the *Cowan* program. Gaussian analytical expressions with four exponential terms are fitted to the values for rare earth elements and the fitted coefficients are tabulated. The tables can be used to interpret the form factor measurements for rare earth metals. Using the radial integrals of Ce 4f and 5d electrons, the experimental measurement of the magnetic form factor of CePd$_3$ is investigated.

1. Introduction

Rare earth elements have attracted many researchers because of their specific magnetic properties (Jensen & Mackintosh, 1991). Rare earth magnets such as Sm–Co and Nd–Fe–B have larger magnetic moments than conventional ferrite or ceramic magnets. The large magnetic moments of rare earth magnets are widely applied to current electronic devices. Although the 4f electrons of rare earth magnets contribute to the magnetic properties in many cases, the 5d electrons may also add to the magnetic properties. For example, Ce compounds have attracted attention because of localized 4f and delocalized 5d electrons. These compounds appear to have magnetic moments originating from both sets of electrons.

Several experiments have been performed to investigate the magnetic properties of rare earth magnets and have revealed the contribution arising from 5d electrons to magnetic structures. The magnetic form factor contributed from Ce 5d electrons in CeRh$_3$B$_2$ was investigated by polarized neutron diffraction (Alonso *et al.*, 1998; Givord, Boucherle *et al.*, 2004; Givord *et al.*, 2007), magnetic Compton scattering (Yaouanc *et al.*, 1998; Galatanu *et al.*, 2003; Sakurai *et al.*, 2003) and X-ray magnetic diffraction (Ito *et al.*, 2012). A polarized neutron study demonstrated that a magnetic form factor of CePd$_3$ might include a contribution from Ce 5d electrons in addition to that from Ce 4f electrons at low temperatures (Stassis *et al.*, 1982; Givord, Galéra *et al.*, 2004). X-ray magnetic circular dichroism (XMCD) experiments on RFe$_2$ (R = Ce, Lu, Hf, Gd) showed that R 5d electrons in RFe$_2$ could be polarized owing to the interaction between R 5d and Fe 3d electrons (Giorgetti *et al.*, 1993). Polarized neutron diffraction showed that RFe$_2$ (R = Ce, Lu) had 5d magnetic moments (Murani, 2004). The Eu L_3-edge XMCD revealed that the Eu 5d spin polarization in Eu$_{0.95}$Fe$_4$Sb$_{12}$ could be enhanced as a result of the inter-atomic exchange interaction with Fe 3d bands (Krishnamurthy *et al.*, 2009). These studies suggest that, in addition to 4f electrons, 5d electrons contribute to the magnetic structure of some rare earth compounds.

The magnetic form factor can be observed and analysed to model magnetic structures. Polarized neutron diffraction (PND) has provided a traditional probe for magnetic form factor measurements (Bacon, 1975; Lovesey, 1986; Williams, 1988). Owing to the availability of brilliant X-ray sources, X-ray magnetic diffraction (XMD) has enabled us to measure the spin and orbital contributions of the magnetic form factor separately (Blume, 1985; Lovesey, 1987; Blume & Gibbs, 1988). Using an elliptically polarized white X-ray beam, the experimental accuracy of XMD has become comparable to that of PND (Laundy *et al.*, 1991; Collins *et al.*, 1992; Ito *et al.*, 1995, 2004; Suzuki *et al.*, 2009).

In an analysis of the measured magnetic form factor for studying magnetic structures and magnetic moments, the atomic model is frequently used when the magnetic electrons are considered to be localized. For this atomic model, the radial integrals, $\langle j_L \rangle$, are used to interpret the experimental results. In practical applications, approximated Gaussian analytical expressions for $\langle j_L \rangle$ are widely used. The functional forms of the expressions are parameterized by several fitting parameters. The coefficients were fitted to Gaussian analytical expressions with three exponential terms for the 3d and 4d electrons of transition atoms and ions, the 4f electrons of rare earth ions and the 5f electrons of actinide ions, and these were tabulated (Brown, 2004). Recently, the values of the radial integrals for the 5d electrons of transition atoms and ions have been calculated and the fitted parameters in the Gaussian analytical expressions with four exponential terms were tabulated (Kobayashi *et al.*, 2011). Up to now, a table of the radial integrals for the 5d electrons of rare earth elements has been absent. Because of this absence, the magnetic form factor study of rare earth magnets may have been limited.

The purpose of this paper is to calculate $\langle j_L \rangle$ values to describe the magnetic form factor for the 5d electrons of rare

Table 1
$\langle j_0 \rangle$ form factors of the $5d$ electrons of rare earth ions.

Ions (electronic configuration)	A_0	a_0	B_0	b_0	C_0	c_0	D_0	d_0	E_0	e
La^{2+} ($4f^05d^1$)	0.5488	63.822	0.7238	34.429	−6.0375	7.092	5.7655	6.839	−0.0008	0.0810
Ce^{2+} ($4f^15d^1$)	0.4959	63.797	0.7571	34.334	−5.9903	6.595	5.7381	6.370	−0.0009	0.0693
Ce^{3+} ($4f^05d^1$)	1.2395	35.447	−1.6420	4.939	1.9467	3.715	−0.5481	2.671	0.0020	0.0813
Pr^{2+} ($4f^25d^1$)	0.4568	63.765	0.7795	34.094	−5.1096	6.186	4.8743	5.950	−0.0011	0.0584
Pr^{3+} ($4f^15d^1$)	0.7735	40.670	0.6284	21.775	−7.2962	6.114	6.8955	5.866	−0.0015	0.0754
Pr^{4+} ($4f^05d^1$)	1.3076	27.762	−3.2363	4.278	4.3424	3.471	−1.4168	2.758	0.0018	0.0594
Nd^{2+} ($4f^35d^1$)	1.2972	27.071	−2.4336	4.208	3.2415	3.271	−1.1081	2.568	0.0016	0.0626
Nd^{3+} ($4f^25d^1$)	0.6179	41.924	0.7344	23.743	−5.2140	5.726	4.8631	5.427	−0.0016	0.0628
Nd^{4+} ($4f^15d^1$)	1.2972	27.071	−2.4336	4.208	3.2415	3.271	−1.1081	2.568	0.0016	0.0626
Pm^{3+} ($4f^35d^1$)	0.5149	42.825	0.8077	24.559	−3.6851	5.432	3.3642	5.053	−0.0018	0.0517
Sm^{2+} ($4f^55d^1$)	0.3908	63.383	0.8062	32.974	−5.5271	5.174	5.3313	5.015	−0.0013	0.0319
Sm^{3+} ($4f^45d^1$)	0.4725	42.826	0.8301	24.562	−3.0608	5.170	2.7600	4.755	−0.0019	0.0421
Eu^{2+} ($4f^65d^1$)	0.3827	63.023	0.8044	32.481	−1.8540	5.066	1.6682	4.618	−0.0014	0.0255
Eu^{3+} ($4f^55d^1$)	0.3784	44.430	0.9025	25.126	−1.3521	4.871	2.8731	4.511	−0.0020	0.0335
Gd^{+} ($4f^85d^1$)	0.4982	104.440	0.5928	44.451	−14.5061	4.692	14.4155	4.664	−0.0008	0.0200
Gd^{+} ($6s^14f^75d^1$)	0.4132	75.211	0.7389	33.606	−1.8951	4.755	1.7441	4.411	−0.0013	0.0200
Gd^{2+} ($4f^75d^1$)	0.3745	62.755	0.8026	32.071	−8.6327	4.644	8.4569	4.560	−0.0014	0.0199
Gd^{3+} ($4f^65d^1$)	0.3587	44.300	0.9082	24.875	−2.6769	4.664	2.4120	4.274	−0.0020	0.0271
Gd^{4+} ($4f^55d^1$)	0.4512	32.712	0.9183	19.602	−2.8665	4.569	2.4997	4.098	−0.0027	0.0319
Tb^{+} ($4f^95d^1$)	0.5057	104.335	0.5796	43.869	−1.6061	4.572	1.5212	4.339	−0.0008	0.0193
Tb^{+} ($6s^14f^95d^1$)	0.4131	74.925	0.7311	33.131	−1.2648	4.612	1.1216	4.133	−0.0013	0.0168
Tb^{2+} ($4f^85d^1$)	0.3734	62.276	0.7955	31.562	−3.4780	4.492	3.3105	4.298	−0.0014	0.0159
Tb^{3+} ($4f^75d^1$)	0.3223	44.892	0.9303	24.826	−3.9948	4.375	3.7443	4.140	−0.0021	0.0204
Tb^{4+} ($4f^65d^1$)	0.3614	33.730	0.9844	19.945	−2.6536	4.355	2.3105	3.892	−0.0028	0.0250
Dy^{2+} ($4f^95d^1$)	0.3754	61.715	0.7859	31.049	−1.7452	4.388	1.5853	4.024	−0.0014	0.0131
Dy^{3+} ($4f^85d^1$)	0.3014	45.110	0.9392	24.622	−3.2549	4.203	3.0163	3.936	−0.0021	0.0158
Ho^{3+} ($4f^95d^1$)	0.2974	44.755	0.9335	24.262	−2.3286	4.079	2.0998	3.728	−0.0021	0.0127
Er^{3+} ($4f^{10}5d^1$)	0.2916	44.550	0.9304	23.933	−1.3854	4.035	1.1655	3.468	−0.0021	0.0103
Tm^{2+} ($4f^{12}5d^1$)	0.4067	59.305	0.7386	29.168	−0.3795	4.593	0.2356	2.956	−0.0015	0.0082
Tm^{3+} ($4f^{11}5d^1$)	0.3302	42.750	0.8905	23.057	−0.5894	4.397	0.3708	2.923	−0.0022	0.0086
Tm^{4+} ($4f^{10}5d^1$)	0.2406	35.005	1.0453	19.560	−4.5727	3.572	4.2895	3.383	−0.0027	0.0087
Yb^{2+} ($4f^{13}5d^1$)	0.4170	58.627	0.7233	28.615	−0.3308	4.553	0.1919	2.742	−0.0015	0.0078
Yb^{3+} ($4f^{12}5d^1$)	0.3498	41.749	0.8666	22.455	−0.4923	4.434	0.2780	2.671	−0.0022	0.0078
Lu^{2+} ($4f^{14}5d^1$)	0.4216	58.262	0.7131	28.218	−0.3048	4.446	0.1715	2.593	−0.0015	0.0078
Lu^{3+} ($4f^{13}5d^1$)	0.3217	42.404	0.8845	22.448	−0.4726	4.258	0.2686	2.566	−0.0022	0.0064

earth elements. These values are important in finding magnetic contributions from individual atoms in rare earth magnets. As an example of a practical application of these radial integrals, we revisit the magnetic form factor of CePd$_3$ where the contribution from the Ce $5d$ electrons, in addition to that from the Ce $4f$ electrons, has been suggested (Stassis et al., 1982).

The remainder of this paper is organized as follows. In §2, the formalism of the calculation and fitting method is described. In §3, our results for the radial integrals of the $5d$ electrons of rare earth elements are presented and fitted parameters in the Gaussian analytical expressions are tabulated. Finally, an application to the magnetic form factor measurement of CePd$_3$ is presented. In §4, we summarize our research.

2. Method of calculation

The magnetic form factor for the unpaired electrons with quantum number nl in the non-relativistic framework is expressed as

$$F(\mathbf{k}) = \mu \left[\langle j_0(k) \rangle + \sum_{L=2}^{2l} c_L \langle j_L(k) \rangle \right], \qquad (1)$$

where $\mathbf{k}$ is the scattering vector, μ is the total magnetic moment and the summation is taken for the values 2, ..., $2l$. The coefficients c_L generally depend on electronic configurations and experimental conditions (Freeman et al., 1976). The radial integrals for the unpaired electrons using the radial wavefunction $R_{nl}(r)$ are defined by

$$\left\langle j_L \left(s = \frac{k}{4\pi} \right) \right\rangle = \int_0^\infty R_{nl}^2(r) j_L(kr) r^2 \, \mathrm{d}r, \qquad (2)$$

where $j_L(kr)$ is the spherical Bessel function of the Lth order and the length of the scattering vector is denoted by $k = 4\pi s = (4\pi \sin\theta)/\lambda$.

We employ the Hartree–Fock relativistic (HFR) method in the *Cowan* program (Cowan, 1981) to generate the radial wavefunctions of equation (2). In the HFR calculation, the relativistic effects of the mass–velocity and Darwin terms are added to the non-relativistic Hartree–Fock equation while the spin–orbit term is neglected.

We use the Gaussian analytical expressions with four exponential terms to find fitted parameters of the values of the radial integrals from the HFR method (Kobayashi et al., 2011). This follows *International Tables* in Brown (2004), where the Gaussian analytical expressions with three exponential terms were used. For example, we fit the following Gaussian analy-

Table 2
$\langle j_2 \rangle$ form factors of the 5d electrons of rare earth ions.

Ions (electronic configuration)	A_2	a_2	B_2	b_2	C_2	c_2	D_2	d_2	E_2	e
La^{2+} ($4f^0 5d^1$)	12.9681	48.694	9.8018	22.831	−0.5443	4.354	0.2584	2.743	−0.0001	0.0178
Ce^{2+} ($4f^1 5d^1$)	12.6550	47.222	9.3025	21.878	−0.6896	3.762	0.4405	2.849	0.0000	0.0189
Ce^{3+} ($4f^0 5d^1$)	8.7013	35.824	8.5894	18.242	−0.6110	4.306	0.2181	2.336	−0.0003	0.0093
Pr^{2+} ($4f^2 5d^1$)	12.4487	45.891	8.8239	21.010	−17.0630	3.120	16.8417	3.095	0.0001	0.0219
Pr^{3+} ($4f^1 5d^1$)	8.5203	34.877	8.2069	17.602	−0.5841	3.958	0.2347	2.302	−0.0002	0.0107
Pr^{4+} ($4f^0 5d^1$)	6.3910	28.309	7.6746	15.204	−0.6973	4.010	0.2304	2.119	−0.0004	0.0057
Nd^{2+} ($4f^3 5d^1$)	6.2640	27.628	7.3661	14.731	−0.6560	3.743	0.2354	2.073	−0.0003	0.0072
Nd^{3+} ($4f^2 5d^1$)	8.3541	34.036	7.8675	17.031	−0.5998	3.584	0.2896	2.326	0.0000	0.0109
Nd^{4+} ($4f^1 5d^1$)	6.2640	27.628	7.3661	14.731	−0.6560	3.743	0.2354	2.073	−0.0003	0.0072
Pm^{3+} ($4f^3 5d^1$)	8.2028	33.286	7.5637	16.518	−0.8756	3.105	0.6007	2.486	0.0002	0.0116
Sm^{2+} ($4f^5 5d^1$)	12.0956	42.678	7.6076	18.857	−1.4355	2.749	1.2720	2.547	0.0001	0.0268
Sm^{3+} ($4f^4 5d^1$)	8.1212	32.502	7.2340	15.990	−5.8639	2.698	5.6142	2.630	0.0003	0.0136
Eu^{2+} ($4f^6 5d^1$)	12.0033	41.860	7.2896	18.289	−1.4882	2.592	1.3411	2.425	0.0000	0.0288
Eu^{3+} ($4f^5 5d^1$)	8.0653	31.753	6.9151	15.484	−5.5701	2.578	5.3406	2.515	0.0003	0.0143
Gd^{+} ($4f^8 5d^1$)	22.2510	65.913	7.5925	23.045	−3.5803	1.952	3.5355	1.930	−0.0010	0.0818
Gd^{+} ($6s^1 4f^7 5d^1$)	14.0295	48.586	7.3596	18.927	−5.1053	2.242	5.0055	2.211	−0.0004	0.0507
Gd^{2+} ($4f^7 5d^1$)	11.9202	41.129	7.0021	17.772	−5.3982	2.392	5.2663	2.354	−0.0001	0.0315
Gd^{3+} ($4f^6 5d^1$)	8.0082	31.074	6.6281	15.022	−1.9932	2.515	1.7825	2.354	0.0003	0.0146
Gd^{4+} ($4f^5 5d^1$)	5.8839	25.328	6.3297	13.143	−1.1650	2.597	0.8829	2.219	0.0004	0.0077
Tb^{+} ($4f^9 5d^1$)	22.4050	65.581	7.3158	22.565	−4.9513	1.745	4.9149	1.732	−0.0014	0.0880
Tb^{+} ($6s^1 4f^8 5d^1$)	14.0011	48.000	7.0994	18.468	−0.6304	2.188	0.5431	1.960	−0.0007	0.0543
Tb^{2+} ($4f^8 5d^1$)	11.8504	40.480	6.7412	17.303	−11.6794	2.248	11.5615	2.233	−0.0002	0.0339
Tb^{3+} ($4f^7 5d^1$)	7.9534	30.456	6.3665	14.596	−0.8418	2.508	0.6482	2.145	0.0002	0.0158
Tb^{4+} ($4f^6 5d^1$)	5.8406	24.788	6.0831	12.775	−2.0431	2.400	1.7828	2.221	0.0004	0.0088
Dy^{2+} ($4f^9 5d^1$)	11.7905	39.898	6.5024	16.874	−11.5993	2.115	11.4943	2.102	−0.0003	0.0359
Dy^{3+} ($4f^8 5d^1$)	7.8866	29.902	6.1361	14.212	−12.5093	2.229	12.3329	2.210	0.0002	0.0177
Ho^{3+} ($4f^9 5d^1$)	7.8279	29.392	5.9224	13.854	−3.0002	2.151	2.8393	2.080	0.0001	0.0183
Er^{3+} ($4f^{10} 5d^1$)	7.7700	28.922	5.7263	13.523	−4.1104	2.035	3.9640	1.990	0.0000	0.0200
Tm^{2+} ($4f^{12} 5d^1$)	11.6672	38.468	5.8888	15.774	−4.8013	1.717	4.7296	1.697	−0.0012	0.0439
Tm^{3+} ($4f^{11} 5d^1$)	7.7142	28.488	5.5450	13.214	−5.7987	1.923	5.6660	1.895	−0.0002	0.0209
Tm^{4+} ($4f^{10} 5d^1$)	5.6664	23.000	5.2790	11.534	−3.2389	1.988	3.0496	1.919	0.0002	0.0166
Yb^{2+} ($4f^{13} 5d^1$)	11.6437	38.074	5.7103	15.455	−2.9992	1.582	2.9369	1.554	−0.0017	0.0462
Yb^{3+} ($4f^{12} 5d^1$)	7.6609	28.088	5.3775	12.926	−5.9455	1.817	5.8255	1.793	−0.0004	0.0223
Lu^{2+} ($4f^{14} 5d^1$)	11.6308	37.717	5.5427	15.158	−6.0682	1.432	6.0147	1.420	−0.0024	0.0504
Lu^{3+} ($4f^{13} 5d^1$)	7.6106	27.715	5.2212	12.656	−2.1969	1.729	2.0887	1.671	−0.0007	0.0236

tical expressions to the calculated values for $\langle j_L \rangle$ of the 5d electrons:

$$\langle j_L(s) \rangle =$$
$$\begin{cases} A_L \exp(-a_L s^2) + B_L \exp(-b_L s^2) \\ \quad + C_L \exp(-c_L s^2) + D_L \exp(-d_L s^2) + E_L, \quad L = 0 \quad (3) \\ s^2[A_L \exp(-a_L s^2) + B_L \exp(-b_L s^2) \\ \quad + C_L \exp(-c_L s^2) + D_L \exp(-d_L s^2) + E_L], \quad L = 2, 4 \quad (4) \end{cases}$$

where $A_L, a_L, B_L, b_L, C_L, c_L, D_L, d_L, E_L$ are fitting parameters for each value of L. The values of the parameters are determined by minimizing the following value:

$$e = 100 \left(\left\{ \sum_{i=1}^{N} \left[\langle j_L(s_i) \rangle^{HFR} \right. \right. \right.$$
$$\left. \left. \left. - \langle j_L(s_i, A_L, a_L, B_L, b_L, C_L, c_L, D_L, d_L, E_L) \rangle \right]^2 \right\} / N \right)^{1/2},$$
$$(5)$$

where the sum is taken over the computed points used, N is the number of computed points, $\langle j_L(s_i) \rangle^{HFR}$ are the computed values of the radial integrals using HFR, and $\langle j_L(s_i, A_L, a_L, B_L, b_L, C_L, c_L, D_L, d_L, E_L) \rangle$ are expressed as in equations (3) and (4), where the parameter dependence is explicitly expressed. The numerical values of the radial inte-

grals from the HFR method are calculated from 0 to 1.5 Å^{-1} for $s = (\sin \theta)/\lambda$ at an interval of 0.01 Å^{-1}, and then the above Gaussian analytical expressions are fitted to the numerical values.

3. Results and discussion

First, the fitted coefficients of calculated radial integrals are tabulated for possible electronic configurations and valence numbers of the 5d electrons in rare earth metal compounds. Table 1 shows the fitting parameters in equation (3) for $\langle j_0 \rangle$, and Tables 2 and 3 list the fitting parameters in equation (4) for $\langle j_2 \rangle$ and $\langle j_4 \rangle$, respectively. The e values defined by equation (5) are given in these tables. The electronic states with a high valence number may be described more correctly by the Gaussian analytical expressions than those with a low valence number because the fitting parameter e decreases as the valence number increases. This tendency was seen for the calculation of the 5d electrons of transition elements (Kobayashi et al., 2011).

We consider the magnetic form factor of Ce in $CePd_3$, which is a rare earth intermediate-valence compound (Lawrence, 2008) and has the cubic $AuCu_3$-type structure. Stassis et al. (1982) interpreted the observed magnetic form factor of $CePd_3$ at $T = 4.2$ K and argued that it might have contributions

Table 3
$\langle j_4 \rangle$ form factors of the $5d$ electrons of rare earth ions.

Ions (electronic configuration)	A_4	a_4	B_4	b_4	C_4	c_4	D_4	d_4	E_4	e
La^{2+} ($4f^05d^1$)	−4.5158	53.905	3.2057	16.650	6.5227	6.913	−5.0984	6.414	0.0030	0.0432
Ce^{2+} ($4f^15d^1$)	−4.2564	53.290	3.1514	15.564	4.8631	6.428	−3.6555	5.879	0.0029	0.0326
Ce^{3+} ($4f^05d^1$)	−3.4280	40.945	3.4454	9.613	−1.7690	0.878	1.7363	0.845	−0.0112	0.0245
Pr^{2+} ($4f^25d^1$)	−4.0440	52.865	3.1023	14.699	16.7869	5.775	−15.7537	5.659	0.0027	0.0242
Pr^{3+} ($4f^15d^1$)	−3.2801	40.342	3.2838	9.275	−0.3302	0.693	0.3218	0.526	−0.0262	0.0256
Pr^{4+} ($4f^05d^1$)	−3.0144	29.731	3.0921	8.040	−1.7853	1.018	1.7254	0.978	−0.0067	0.0111
Nd^{2+} ($4f^35d^1$)	−2.8914	29.223	2.9558	7.788	−2.3133	0.821	2.2706	0.794	−0.0122	0.0159
Nd^{3+} ($4f^25d^1$)	−3.4188	35.732	2.4046	11.623	4.7757	5.234	−3.6967	4.807	0.0034	0.0210
Nd^{4+} ($4f^15d^1$)	−2.8914	29.223	2.9558	7.788	−1.0406	0.837	0.9980	0.776	−0.0122	0.0123
Pm^{3+} ($4f^35d^1$)	−3.2587	35.415	2.4193	10.957	6.6210	4.804	−5.7219	4.569	0.0033	0.0159
Sm^{2+} ($4f^55d^1$)	−3.5892	52.139	2.9096	13.054	4.6201	4.925	−3.8766	4.647	0.0023	0.0090
Sm^{3+} ($4f^45d^1$)	−3.1219	35.108	2.4059	10.444	4.7313	4.540	−3.9603	4.264	0.0031	0.0117
Eu^{2+} ($4f^65d^1$)	−3.4800	51.945	2.8285	12.745	1.5317	5.052	−0.8219	4.111	0.0022	0.0078
Eu^{3+} ($4f^55d^1$)	−3.0029	34.814	2.3781	10.031	5.4031	4.255	−4.7274	4.056	0.0029	0.0092
Gd$^+$ ($4f^85d^1$)	−4.8713	104.143	3.7302	21.468	1.2023	8.378	−0.0196	2.098	0.0014	0.0130
Gd$^+$ ($6s^14f^75d^1$)	−3.4617	66.516	2.6499	14.221	1.0035	6.279	−0.1055	3.023	0.0019	0.0075
Gd^{2+} ($4f^75d^1$)	−3.3883	51.671	2.7278	12.570	1.0357	5.277	−0.3195	3.576	0.0020	0.0071
Gd^{3+} ($4f^65d^1$)	−2.8981	34.532	2.3381	9.696	4.9222	4.040	−4.3145	3.851	0.0028	0.0077
Gd^{4+} ($4f^55d^1$)	−2.6251	26.189	2.0430	8.166	2.0627	3.948	−1.4456	3.441	0.0034	0.0084
Tb$^+$ ($4f^95d^1$)	−4.8446	105.564	3.7187	21.493	1.1716	8.254	−0.0140	1.741	0.0014	0.0138
Tb$^+$ ($6s^14f^85d^1$)	−3.3986	66.558	2.5566	14.238	0.9966	6.354	−0.0687	2.640	0.0018	0.0064
Tb^{2+} ($4f^85d^1$)	−3.3137	51.300	2.6051	12.543	0.9119	5.572	−0.1465	3.041	0.0019	0.0067
Tb^{3+} ($4f^75d^1$)	−2.8051	34.263	2.2899	9.422	2.9540	3.912	−2.3939	3.623	0.0026	0.0058
Tb^{4+} ($4f^65d^1$)	−2.5322	25.901	2.0176	7.883	1.3901	3.855	−0.8421	3.162	0.0033	0.0075
Dy^{2+} ($4f^95d^1$)	−3.2454	51.015	2.5045	12.508	0.8905	5.686	−0.0924	2.673	0.0019	0.0062
Dy^{3+} ($4f^85d^1$)	−2.7206	34.002	2.2384	9.188	2.3604	3.779	−1.8355	3.448	0.0024	0.0063
Ho^{3+} ($4f^95d^1$)	−2.6442	33.767	2.1895	8.981	6.7096	3.527	−6.2142	3.430	0.0023	0.0047
Er^{3+} ($4f^{10}5d^1$)	−2.5747	33.543	2.1374	8.808	4.3319	3.435	−3.8556	3.294	0.0021	0.0048
Tm^{2+} ($4f^{12}5d^1$)	−3.0741	50.565	2.2967	12.375	0.8709	5.675	−0.0368	1.903	0.0017	0.0045
Tm^{3+} ($4f^{11}5d^1$)	−2.5119	33.318	2.0781	8.676	1.1694	3.573	−0.6974	2.972	0.0020	0.0046
Tm^{4+} ($4f^{10}5d^1$)	−2.2376	24.879	1.8856	7.074	1.9119	3.067	−1.5307	2.802	0.0026	0.0052
Yb^{2+} ($4f^{13}5d^1$)	−3.0265	50.522	2.2491	12.330	0.8621	5.625	−0.0285	1.693	0.0017	0.0058
Yb^{3+} ($4f^{12}5d^1$)	−2.4567	33.073	2.0029	8.603	0.7458	3.803	−0.2541	2.601	0.0019	0.0048
Lu^{2+} ($4f^{14}5d^1$)	−2.9837	50.531	2.2096	12.288	0.8518	5.567	−0.0224	1.492	0.0017	0.0049
Lu^{3+} ($4f^{13}5d^1$)	−2.4054	32.850	1.9337	8.538	0.6672	3.906	−0.1577	2.358	0.0018	0.0049

arising from the $4f$ and $5d$ electrons of Ce. Such a contribution may arise as a result of the relativistic formulation and by using the $4f$ integrals derived from relativistic wavefunctions and $5d$ radial integrals which have been obtained from Dirac–Slater wavefunctions. The accuracy of Dirac–Slater wavefunctions is less than that of HFR wavefunctions or relativistic wavefunctions. Recently, Givord, Galéra *et al.* (2004) have concluded from their magnetic form factor measurement that the contribution of the $5d$ electrons of Ce to the magnetic form factor at $T = 1.7$ K could have been anticipated from the analysis based on the dipole approximation using only $4f$ radial integrals from relativistic wavefunctions (Freeman & Desclaux, 1979).

In order to revisit the experimental data of Givord, Galéra *et al.* (2004), we use the dipole approximation, in which the magnetic form factor F for unpaired localized electrons is expressed as (Balcar & Lovesey, 1989)

$$F_{\text{dipole}}^{nl}(s) = (\mu_{\text{S},nl} + \mu_{\text{L},nl})\langle j_0(s)\rangle + \mu_{\text{L},nl}\langle j_2(s)\rangle, \qquad (6)$$

where $\mu_{\text{S},nl}$ and $\mu_{\text{L},nl}$ are the contributions of the spin and orbital magnetic moments of electrons with the state nl, respectively. We use the following two forms for the magnetic form factor analysis: the dipole approximation in $4f$ electrons, F_{dipole}^{4f}, and the $4f$ dipole approximation with spin contributions

from $5d$ electrons, $F_{\text{dipole}}^{4f} + F_{\text{spin}}^{5d}$. Here F_{spin}^{5d} in equation (6) is obtained with $\mu_{\text{L},5d} = 0$, *i.e.* by assuming the quenching of the orbital angular momentum.

In Table 4 we show the radial integrals of Ce^{3+} $5d$ and $4f$ wavefunctions using the HFR method, evaluated in the $5d^1$ and $4f^1$ configurations, respectively, and these are employed in our magnetic form factor analysis. For the Ce^{3+} $4f^1$ configuration, we get essentially the same values as Freeman & Desclaux (1979). The fitted Gaussian analytical expressions are plotted in Fig. 1 for the Ce^{3+} $5d^1$ configuration with the numerical values of the radial integrals at an interval of 0.05 Å^{-1}. The radial integrals of $5d$ electrons decrease more rapidly as a function of s than those of $4f$ electrons.

To find the best fitting functions, the least-squares fitting method is used (Galassi *et al.*, 2009). $\mu_{\text{S},4f}$ and $\mu_{\text{L},4f}$ are fitting parameters for F_{dipole}^{4f}, and $\mu_{\text{S},4f}$, $\mu_{\text{L},4f}$ and $\mu_{\text{S},5d}$ are parameters for $F_{\text{dipole}}^{4f} + F_{\text{spin}}^{5d}$. The best parameter set is found by minimizing χ^2, which is defined by

$$\chi^2 = \sum_{i=1}^{N_e} w_i(y_i - F)^2, \qquad (7)$$

where N_e is the number of measured experimental points, $w_i = 1/\sigma_i^2$ is the inverse square of the error of the experi-
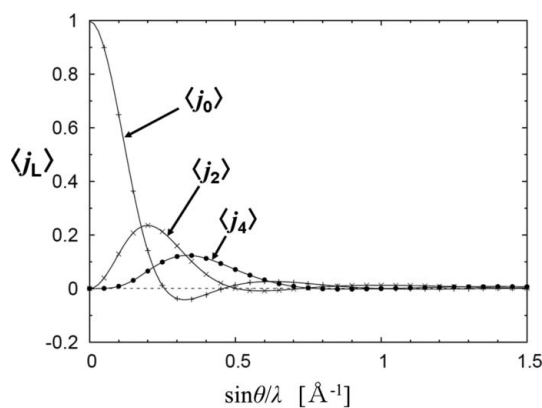
Table 4
The values of radial integrals for Ce^{3+} ($5d$) and Ce^{3+} ($4f$).

$\sin\theta/\lambda$	$\langle j_0\rangle_{5d}$	$\langle j_2\rangle_{5d}$	$\langle j_4\rangle_{5d}$	$\langle j_0\rangle_{4f}$	$\langle j_2\rangle_{4f}$	$\langle j_4\rangle_{4f}$	$\langle j_6\rangle_{4f}$
0.00	1.0000	0.0000	0.0000	1.0000	0.0000	0.0000	0.0000
0.05	0.8989	0.0396	0.0006	0.9763	0.0094	0.0000	0.0000
0.10	0.6488	0.1288	0.0082	0.9097	0.0351	0.0007	0.0000
0.15	0.3648	0.2077	0.0308	0.8117	0.0708	0.0032	0.0001
0.20	0.1415	0.2359	0.0654	0.6969	0.1088	0.0085	0.0006
0.25	0.0124	0.2124	0.0990	0.5786	0.1430	0.0168	0.0016
0.30	−0.0376	0.1595	0.1197	0.4663	0.1696	0.0274	0.0036
0.35	−0.0403	0.1016	0.1233	0.3660	0.1872	0.0394	0.0067
0.40	−0.0230	0.0535	0.1125	0.2800	0.1962	0.0515	0.0108
0.45	−0.025	0.0203	0.0932	0.2086	0.1977	0.0628	0.0156
0.50	0.0135	0.0012	0.0710	0.1509	0.1935	0.0727	0.0209
0.60	0.0266	−0.0086	0.0321	0.0698	0.1735	0.0869	0.0317
0.70	0.0226	−0.0019	0.0087	0.0226	0.1464	0.0936	0.0415
0.80	0.0134	0.0064	−0.0011	−0.0026	0.1185	0.0940	0.0490
0.90	0.0052	0.0113	−0.0025	−0.0144	0.0930	0.0900	0.0539
1.00	0.0002	0.0125	−0.0003	−0.0186	0.0713	0.0832	0.0565
1.10	−0.0019	0.0112	0.0028	−0.0187	0.0536	0.0750	0.0570
1.20	−0.0020	0.0087	0.0052	−0.0169	0.0396	0.0663	0.0559
1.30	−0.0011	0.0060	0.0067	−0.0143	0.0289	0.0577	0.0536
1.40	0.0003	0.0036	0.0072	−0.0116	0.0207	0.0496	0.0505
1.50	0.0016	0.0017	0.0069	−0.0091	0.0146	0.0423	0.0470

mental data σ_i, y_i are the experimental data, and F are the fitted functions, F_{dipole}^{4f} or $F_{dipole}^{4f} + F_{spin}^{5d}$.

Fig. 2 shows the fitted lines with the experimental data of Givord, Galéra *et al.* (2004) at $T = 1.7$ K. The fitted line of F_{dipole}^{4f} deviates from the experimental points, especially for the first two reflections in the region $s < 0.2$ Å^{-1}. The inclusion of the contribution from the $5d$ electron obviously improves the description of the experimental data, in particular in the low-s region; from this we are inclined to conclude that the inclusion of a $5d$ electron contribution is indispensable to get a better fitting of the Ce magnetic form factor at $T = 1.7$ K.

However, since the dipole approximation gives a poor result on several occasions, we should be cautious in deriving a conclusion from the result. To go beyond the dipole approximation for the case of a Ce ion in CePd$_3$, the crystal electric field (CEF) splitting is one of the inevitable factors to be taken into account. The presence of the CEF causes an anisotropic
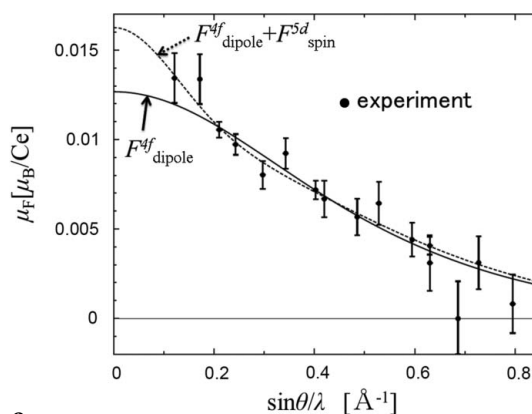
magnetic distribution and the magnetic form factor needs higher-order terms in equation (1) including their angular dependence (Lovesey, 1986; Balcar & Lovesey, 1989). For example, the treatment beyond the dipole approximation on Ce^{3+} in CePd$_2$Si$_2$ improved the form factor significantly, though the dipole approximation still gave an acceptable result at small s (Rotter & Boothroyd, 2009). Another complication involved in the present material is the valence mixing of the Ce $4f$ electron. Several experiments have shown that the Ce ion in CePd$_3$ is considered in the $4f^0$ and $4f^1$ configurations (Kanai *et al.*, 2001). Although the effect of the valence mixing is phenomenologically taken into account in our treatment by including the $5d$ as well as $4f$ radial integrals (Kennedy *et al.*, 1993), more sophisticated theory should be employed for the correct description of the valence mixing state (Lawrence, 2008; Ayuel & de Châtel, 2000). Inclusion of these complications beyond the dipole approximation is intriguing and needs to be tackled in a future study.

4. Conclusions

The radial integrals of the $5d$ electrons of rare earth ions were calculated using the HFR method in the *Cowan* program and the fitted coefficients in the Gaussian analytical expressions were tabulated. The table of the coefficients in the Gaussian analytical expressions can be used for the interpretation of magnetic form factor measurements of the $5d$ electrons in rare earth magnets.

In order to exemplify the utility of our calculated table, the radial integrals of the Ce^{3+} ion were used to analyse the experimental magnetic form factor of CePd$_3$ and the contributions from the $4f$ and $5d$ electrons of Ce were studied. The fitting shows that the $5d$ electrons may play a critical role in the measured magnetic form factor. In summary, inclusion of the $5d$ contribution may open up a new possibility to describe the magnetic properties of other rare earth magnets. Our research may help in the study of these magnets.

Figure 1
Comparison between the analytical expressions using the coefficients in the table (lines) and the calculated values (+ for $\langle j_0\rangle$, × for $\langle j_2\rangle$, ● for $\langle j_4\rangle$) of the radial integrals of the Ce^{3+} $5d^1$ configuration. The calculated values are plotted at intervals of 0.05 Å^{-1}.

Figure 2
Ce magnetic form factor at $T = 1.7$ K in CePd$_3$. Dots (●) are experimental data with errors in Givord, Galéra *et al.* (2004), where the magnetization measurement was 0.0143 (2) μ_B/Ce. The solid (F_{dipole}^{4f}) and dashed ($F_{dipole}^{4f} + F_{spin}^{5d}$) lines are different fittings to the Ce magnetic form factor.

research papers

References

Alonso, J. A., Boucherle, J. X., Givord, F., Schweizer, J., Gillon, B. & Lejay, P. (1998). *J. Magn. Magn. Mater.* **177–181**, 1048–1049.

Ayuel, K. & de Châtel, P. F. (2000). *Phys. Rev. B*, **61**, 15213.

Bacon, G. E. (1975). *Neutron Diffraction.* Oxford University Press.

Balcar, E. & Lovesey, S. W. (1989). *Theory of Magnetic Neutron and Photon Scattering.* Oxford University Press.

Blume, M. (1985). *J. Appl. Phys.* **57**, 3615–3618.

Blume, M. & Gibbs, D. (1988). *Phys. Rev. B*, **37**, 1779–1789.

Brown, P. J. (2004). *Magnetic form factors. International Tables for Crystallography*, Vol. C, *Mathematical, Physical and Chemical Tables*, 3rd ed., pp. 454–461. Dordrecht: Kluwer Academic Publishers.

Collins, S. P., Laundy, D. & Rollason, A. J. (1992). *Philos. Mag. B***65**, 37–46.

Cowan, R. (1981). *The Theory of Atomic Structure and Spectra.* Berkeley: University of California Press.

Freeman, A. J. & Desclaux, J. P. (1979). *J. Magn. Magn. Mater.* **12**, 11–21.

Freeman, A. J., Desclaux, J. P., Lander, G. H. & Faber, J. (1976). *Phys. Rev. B*, **13**, 1168–1176.

Galassi, M., Davies, J., Theiler, J., Gough, B., Jungman, G., Alken, P., Booth, M. & Rossi, F. (2009). *GNU Scientific Library Reference Manual*, 3rd ed., pp. 443–454. Bristol: Network Theory Limited.

Galatanu, A., Yamamoto, E., Okubo, T., Yamada, M., Thamizhavel, A., Takeuchi, T., Sugiyama, K., Inada, Y. & Onuki, Y. (2003). *J. Phys. Condens. Matter*, **15**, S2187–S2191.

Giorgetti, C., Pizzini, S., Dartyge, E., Fontaine, A., Baudelet, F., Brouder, C., Bauer, P., Krill, G., Miraglia, S., Fruchart, D. & Kappler, J. P. (1993). *Phys. Rev. B*, **48**, 12732–12742.

Givord, F., Boucherle, J. X., Lelievre-Berna, E. & Lejay, P. (2004). *J. Phys. Condens. Matter*, **16**, 1211–1230.

Givord, F., Boucherle, J. X., Murani, A. P., Bewley, R., Galera, R. M. & Lejay, P. (2007). *J. Phys. Condens. Matter*, **19**, 506210.

Givord, F., Galéra, R. M., Murani, A. P. & Lelièvre-Berna, E. (2004). *Physica B*, **350**, E103–E105.

Ito, M., Itoh, F., Tanaka, Y., Koizumi, A., Sakurai, H., Ohata, T., Mori, K., Ochiai, A. & Kawata, H. (1995). *J. Phys. Soc. Jpn*, **64**, 2333–2337.

Ito, M., Nagayasu, R., Tadenuma, T., Suzuki, K., Sato, A., Adachi, H., Sakurai, Y. & Ōnuki, Y. (2012). *Key Eng. Mater.* **497**, 3–7.

Ito, M., Tsuji, N., Itoh, F., Adachi, H., Arakawa, E., Namikawa, K., Nakao, H., Murakami, Y., Taguchi, Y. & Tokura, Y. (2004). *J. Phys. Chem. Solids*, **65**, 1993–1997.

Jensen, J. & Mackintosh, A. R. (1991). *Rare Earth Magnetism: Structures and Excitations.* Oxford University Press.

Kanai, K., Kiss, T., Yokoya, T., Schmerber, G., Kappler, J. P., Parlebas, J. C. & Shin, S. (2001). *J. Electron Spectrosc.* **114**, 741–745.

Kennedy, S. J., Brown, P. J. & Coles, B. R. (1993). *J. Phys. Condens. Matter*, **5**, 5169–5178.

Kobayashi, K., Nagao, T. & Ito, M. (2011). *Acta Cryst.* A**67**, 473–480.

Krishnamurthy, V. V., Keavney, D. J., Haskel, D., Lang, J. C., Srajer, G., Sales, B. C., Mandrus, D. G. & Robertson, J. L. (2009). *Phys. Rev. B*, **79**, 014426.

Laundy, D., Collins, S. P. & Rollason, A. J. (1991). *J. Phys. Condens. Matter*, **3**, 369–372.

Lawrence, J. (2008). *Mod. Phys. Lett. B*, **22**, 1273–1295.

Lovesey, S. W. (1986). *Theory of Neutron Scattering from Condensed Matter.* Oxford University Press.

Lovesey, S. W. (1987). *J. Phys. C*, **20**, 5625–5639.

Murani, A. (2004). *Physica B*, **345**, 89–92.

Rotter, M. & Boothroyd, A. T. (2009). *Phys. Rev. B*, **79**, 140405.

Sakurai, Y., Itou, M., Tamura, J., Nanao, S., Thamizhavel, A., Inada, Y., Galatanu, A., Yamamoto, E. & Onuki, Y. (2003). *J. Phys. Condens. Matter*, **15**, S2183–S2186.

Stassis, C., Loong, C.-K., Zarestky, J., McMasters, O. D., Moon, R. M. & Thompson, J. R. (1982). *J. Appl. Phys.* **53**, 7890–7892.

Suzuki, K., Ito, M., Tsuji, N., Adachi, H. & Kawata, H. (2009). *Jpn. J. Appl. Phys.* **48**, 056506.

Williams, W. G. (1988). *Polarized Neutrons.* Oxford University Press.

Yaouanc, A., Dalmas de Réotier, P., Sanchez, J. P., Tschentscher, T. & Lejay, P. (1998). *Phys. Rev. B*, **57**, R681–R684.